EARLY STAGE EXPERIMENT
Science Description

Experiment/Module: Analysis of Intensity Change Processes Experiment (AIPEX)

Investigator(s): Rob Rogers (Co-PI), Jon Zawislak (Co-PI), Trey Alvey (Co-PI), Jason Dunion (Co-PI), Ghassan Alaka (Co-PI), Heather Holbach (Co-PI), Xiaomin Chen (Co-PI), Josh Wadler (Co-PI, UM/RSMAS)

Requirements: TD, TS, Category 1

Early Stage Science Objective(s) Addressed:

1) Collect datasets that can be used to improve the understanding of intensity change processes, as well as the initialization and evaluation of 3-D numerical models, particularly for TCs experiencing moderate vertical wind shear [*IFEX Goals 1, 3*]

Motivation: While some improvements in operational tropical cyclone (TC) intensity forecasting have been made in recent years (DeMaria et al. 2014), predicting changes in TC intensity (as defined by the 1-min. maximum sustained wind) remains problematic. In particular, the operational prediction of rapid intensification (RI) has proven to be especially difficult (Kaplan et al. 2010). The significant impact of such episodes has prompted the Tropical Prediction Center/National Hurricane Center (TPC/NHC) to declare it as its top forecast priority (Rappaport et al. 2009).

Processes that govern TC intensification span spatial and temporal scales from the environmental to vortex to convective and smaller scales. Recent work has focused on the precipitation distribution and structure to assess regimes associated with TC intensification. Studies using airborne Doppler radar (Rogers et al. 2013) and passive microwave satellite (e.g., Alvey et. al 2015; Tao and Jiang 2015) observations have compared the inner-core structure of intensifying and non-intensifying TCs. Precipitation and deep convection in intensifying cases were found to be more symmetrically distributed and located preferentially inside the radius of maximum wind (RMW) compared to non-intensifying cases. Predictability of the azimuthal and radial distribution of precipitation and deep convection within TCs, however, remains low. Thus, identifying and understanding the environmental and internal (within the inner core) mechanisms that govern the azimuthal and radial distribution of precipitation and deep convection could improve the understanding of the intensification process. Recent studies indicate that these mechanisms may include: the interaction of the vortex with environmental vertical wind shear and dry air, vortex-scale subsidence, surface enthalpy fluxes from the underlying ocean, tropospheric stability, as well as precipitation mode (i.e., shallow, moderately deep, and deep convection, as well as stratiform rain) and the accompanying areally-averaged vertical mass flux profile.

The goal of this experiment is to collect datasets that can be used to: 1) improve the initialization and evaluation of 3-D numerical models; 2) improve the understanding of intensification processes across multiple scales, with particular focus on the mechanisms that govern the azimuthal and radial distribution of precipitation and deep convection. TCs that are experiencing moderate vertical wind shear (5–10 m s^{-1}) over a deep layer (850–200 hPa) are of particular interest, since

EARLY STAGE EXPERIMENT
Science Description

---

this range of shear values is often associated with considerable uncertainty with respect to the prospect for TC intensification (Bhatia and Nolan 2013). The overarching goal is to improve the ability to predict the timing and magnitude of intensification, particularly RI, events.

Background: Prior studies have found a number of large-scale environmental factors that are generally favorable for TC intensification, including low environmental vertical wind shear, high ocean heat content, and elevated low- to mid-tropospheric humidity. Thus far, statistically-based prediction schemes that employ predictors derived from large-scale environmental fields and GOES infrared satellite imagery have generally been shown to provide the most skillful objective RI guidance (Kaplan et al. 2015). These schemes include the SHIPS rapid intensification index (SHIPS-RII) (Kaplan et al. 2010) and the more recently developed Bayesian and logistic regression RI models (Rozoff and Kossin 2011). Kaplan et al. (2015) showed that these statistical models are capable of explaining roughly 20% of the skill of Atlantic basin RI forecasts at a lead-time of 24-h. The remaining 80% of the skill not explained by the statistical models is assumed to be attributable either to processes not explicitly accounted for by those models or by limitations in the predictability of RI events.

On the vortex-scale, a number of observational studies have found that intensifying TCs have more precipitation and convective bursts occur within the high inertial stability region inside the RMW (e.g., Rogers et al. 2013, 2015, 2016). This configuration is favorable for TC intensification for two hypothesized reasons: 1) In the high inertial stability region, heat energy is much more efficiently converted to kinetic energy (Schubert and Hack 1982; Vigh and Schubert 2009), and 2) Diabatic heating within the high inertial stability region enables angular momentum surfaces to be drawn inward at the RMW, resulting in tangential wind spinup (Smith and Montgomery 2016).

Observational studies have also found that intensifying TCs typically have more symmetrically distributed precipitation and deep convection than non-intensifying TCs (e.g., Rogers et al. 2013; Alvey et al. 2015; Tao and Jiang 2015). This is consistent with idealized modeling studies that show that TC intensification is most sensitive to the axisymmetric, azimuthal wavenumber-0 component of diabatic heating (e.g., Nolan et al. 2007). One principal environmental factor that can prevent the development of this symmetry is vertical wind shear. The interaction of TCs with environmental vertical wind shear typically results in a wavenumber-1 asymmetry in vertical motion and precipitation, in which upward vertical motion and deep convection is favored in the downshear semicircle, while downward motion and suppression of deep convection is observed in the upshear semicircle (e.g., Marks et al. 1992; Reasor et al. 2013; Rogers et al. 2016; Zawislak et al. 2016). An increase in asymmetry can lead to the decrease in the projection of diabatic heating onto the axisymmetric, azimuthal wavenumber-0 component that has been shown to be important for TC intensification. However, the magnitude of this asymmetry can exhibit considerable variability, particularly within the moderate shear regime (5–10 m s^{-1}) that has been shown to be problematic for operational intensity forecasts (Bhatia and Nolan 2013). This suggests the importance of understanding what governs the azimuthal distribution of precipitation and deep convection.

EARLY STAGE EXPERIMENT
Science Description

Recent studies have used airborne Doppler radar and dropsonde data to examine what hinders the development of precipitation symmetry in sheared TCs (Rogers et al. 2016; Zawislak et al. 2016; Nguyen et al. 2017). These studies show evidence for several potential hindering factors. First, convective downdrafts associated with the downshear convection can cool and stabilize the lower troposphere in the left of shear and upshear quadrants. Second, subsidence in the upshear quadrants can increase the temperature and decrease the relative humidity of the mid-troposphere, effectively capping the lower troposphere. Third, dry air can be transported laterally from the environment into the TC's upshear quadrants. These hindering factors could be mitigated through several potential mechanisms, as listed in the hypotheses below.

Hypotheses: The following hypotheses will guide the sampling strategies for TCs that have the potential to undergo (rapid) intensification:

1. Intensification is favored when precipitation and deep convection are distributed symmetrically and located preferentially inside the radius of maximum wind (RMW).
2. The local kinematic (e.g., location and depth of radial inflow, vertical alignment of the vortex) and thermodynamic forcing (e.g., SST, available moisture, and RH) are key in governing whether precipitation (deep convection) is symmetrically distributed and primarily inside the radius of maximum wind (RMW)
3. Symmetry is favored when: (a) the mid-troposphere is moistened upshear due to detrainment from mid-tropospheric congestus, evaporation of falling stratiform rain, or reduced lateral advection of dry air from the environment; (b) the lower troposphere is convectively unstable in the upshear quadrants due to enhanced surface enthalpy fluxes from the underlying ocean and/or reduced convective downdrafts.

Aircraft Pattern/Module Descriptions (see *Flight Pattern* document for more detailed information): Missions will be targeted for systems that have a reasonable chance of undergoing intensification based on statistical and numerical model forecast guidance. When possible (i.e., subject to range, timing, and other logistical constraints), missions will begin at least 24 h prior to the expected onset of intensification, while the TC is still at tropical depression or tropical storm intensity. This enables the documentation of TC structure during the time leading up to intensification onset (if it indeed occurs). Ideally missions will continue every 12 h, as long as feasible. If either the P-3 or G-IV aircraft cannot fly every 12 h the experiment can still be conducted provided that the gap between missions for any one of the two aircraft does not exceed 24 h. Although all intensification rates are of interest, priority will be given to those with a high potential for RI according to model guidance and/or are forecast to experience at least moderate (5–10 m s^{-1}) vertical wind shear over a deep layer. There are a few possible configurations for the execution of this experiment, as outlined below:

> **1. Both P-3 and G-IV are available:** This is the optimal configuration for this experiment as, under this scenario, the P-3 and G-IV would coordinate operations (i.e., takeoff times would allow both aircraft to sample the TC simultaneously). The P-3 will sample the inner-core with the standard rotated Figure-4 pattern (P-3 Module 1), while the G-IV will sample the outer environment and near-TC environment (typically around 60 n mi, or 100 km)

with either the circumnavigation (G-IV Module 1) or star (G-IV Module 2) pattern.

2. Only P-3 is available: When the G-IV is not available for coordinated operations, either because of operational tasking requirements or aircraft unavailability, P-3 targeted observations in the near environment and inner core can still contribute towards the objectives of the experiment. In this scenario there are two possible strategies for sampling, which depend on whether the precipitation distribution is asymmetric:

a. TC is highly asymmetric:
This option will be chosen when the precipitation distribution in the targeted TC is expected to be highly asymmetric during the mission. Such an asymmetric configuration would allow for a high-altitude P-3 circumnavigation pattern to at least target the precipitation-free upshear semicircle, and when hazard avoidance is possible the downshear quadrants. Indications of an appropriate magnitude of asymmetry may include:

1) Visible, infrared, or microwave satellite imagery indicates an exposed or partially-exposed low level circulation center (see example below).
2) The environmental vertical wind shear, as indicated by SHIPS, is expected to be sufficient (> 5 m s^{-1}) during the mission to result in an asymmetric precipitation structure.
3) High-resolution numerical guidance (i.e. HWRF) forecast a lack of precipitation in the upshear semicircle of the TC during the mission.
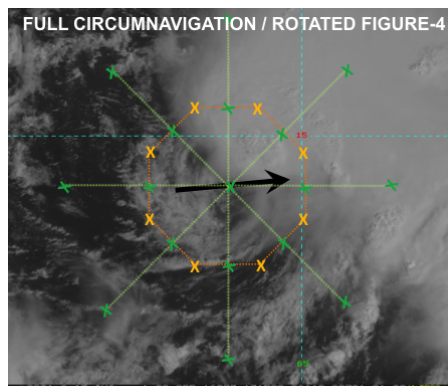

Figure-4 in green, circumnavigation in orange, shear vector in black, 'X' is a dropsonde location).

Given this scenario, the P-3 will sample the near environment and inner core with a pattern that includes a high-altitude circumnavigation and, optimally, a rotated Figure-4 (P-3 Module 2). If time doesn't permit for a complete rotated Figure-4, then a single Figure-4 can be substituted. The radius of the circumnavigation should be as close to the inner-core precipitation shield as safety allows, as best determined through available visible or infrared satellite, microwave, or radar imagery. The high-altitude circumnavigation allows

for increased azimuthal and vertical dropsonde data coverage, particularly in the critical, precipitation-free upshear region that may fill in as intensification commences.

b. TC is relatively symmetric:

This scenario applies to a targeted TC that has the potential for intensification, but the precipitation is expected to be too symmetric during the mission for the P-3 high-altitude circumnavigation to be conducted safely. Here, the P-3 will sample the inner-core vortex structure with the standard rotated Figure-4 pattern (P-3 Module 1).

3. Only G-IV is available: This option is less preferable as targeted observations of the vortex structure are also important towards the objectives of the experiment. This option applies to any targeted TC that has the potential for intensification, regardless of asymmetric structure. Under this option, the G-IV will sample the outer and near environments with either the circumnavigation (G-IV Module 1) or star (G-IV Module 2), and requires that hazard avoidance permit the G-IV to obtain measurements within/very near the inner core.

Links to Other Early Stage Experiments/Modules: If the opportunity arises during the execution of AIPEX, fly the Convective Burst Module or Arc Cloud Module (see accompanying discussion in Field Program plan). The Convective Burst Module would be optimal for determining the structure and evolution of deep convection within the framework of the broader vortex-scale circulation as it interacts with vertical shear (if appropriate), while the Arc Cloud Module would be ideal for documenting locations within the vortex circulation encountering significant low-to mid-level dry air and determining the impact of the associated outflow boundaries on the boundary layer temperature and moisture distribution. The collection of data from the Doppler Wind Lidar (DWL), as a part of the DWL Module, would optimally provide information on the wind field in the absence of radar scatterers, e.g., on the upshear side of the TC. AIPEX can also be flown in conjunction with the following *Early Stage* experiments and modules: SFMR Module, TDR Experiment, Synoptic Flow Experiment, NESDIS JPSS Satellite Validation Experiment, and ADM-Aeolus Satellite Validation Module.

Analysis Strategy: The general analysis strategy follows that performed in recent observational studies (Reasor et al. 2013; Zhang et al. 2013; Rogers et al. 2016; Zawislak et al. 2016; Nguyen et al. 2017). The analysis strategy includes assessing and documenting the time evolution of the following:
- *Azimuthal and radial distribution of inner-core precipitation and deep convection* (P-3 TDR/LF, possibly G-IV TDR). The inner-core precipitation asymmetry, and its projection onto the axisymmetric, azimuthal wavenumber-0 component will be assessed quantitatively (assuming sufficient azimuthal coverage). The location of precipitation and convective bursts relative to the RMW will be examined.
- *Precipitation mode, particularly upshear* (P-3 TDR/LF, possibly G-IV TDR). An analysis of the precipitation mode (shallow, moderately deep, deep convection, as well as stratiform rain), using the vertical velocity and reflectivity structure, will allow for an assessment as

to whether moistening of the inner core occurs through upscale growth of convection (moistening from convective detrainment at gradually higher altitudes), or from the top-down via stratiform rain as hydrometeors produced downshear are transported azimuthally upshear.

- *Structure of the areally-averaged vertical mass flux profiles* (P-3 TDR, possibly G-IV TDR). Literature (Raymond et al. 2011; Gjorgjievska and Raymond 2014) has identified a key transition from a "top heavy" vertical mass flux profile (convergence preferentially in the midtroposhere) to a "bottom heavy" profile (convergence preferentially in the low troposphere) in the development of a TC. To further understand this evolution, the relationship between the mass flux profiles and the contributions of various precipitation modes (through vertical velocity, reflectivity) to overall precipitation will be analyzed.

- *Low-wavenumber thermodynamic and kinematic structure of the boundary layer* (P-3/G-IV dropsondes, DWL for kinematic only). The thermodynamic focus will be on the boundary layer cooling by convective downdrafts and the subsequent recovery via surface enthalpy fluxes from the underlying ocean in the downstream (upshear-left through downshear-right) quadrants. Surface enthalpy fluxes will be calculated where dropsondes are paired with AXBTs that provide sea surface temperature. The kinematic focus will be on obtaining measurements of the strength and depth of boundary layer inflow and convergence in the boundary layer, both in a symmetric sense and relative to the shear vector (when relevant). Additionally, the gradient and agradient flow in the boundary layer will be calculated.

- *Low-wavenumber thermodynamic and kinematic structure above the boundary layer* (P-3/G-IV dropsondes, P-3/G-IV TDR and DWL for kinematic only). The presence of mid-tropospheric dry air is of particular interest. Assuming mid-tropospheric dry air is present (most likely in the upshear quadrants), the potential sources of this dry air (vortex-scale subsidence or lateral advection from the environment) and how this upshear dry air is removed (i.e., through detrainment from congestus or evaporation of stratiform precipitation) will be assessed.

- *Vortex tilt* (P-3 TDR, possibly G-IV TDR). Assuming sufficient TDR coverage, the vortex tilt will be examined quantitatively by merging TDR analyses from each Figure-4. If the vortex tilt appears to decrease rapidly during a flight, individual TDR analyses can be used to qualitatively examine the time evolution of vortex tilt during the alignment process.

- *Vertical wind shear and upper-level divergence* (G-IV dropsondes). These quantities will be computed and compared with global model analyses. The vertical distribution of shear will also be evaluated, as upper-level shear is hypothesized to be less deleterious than low-level shear.

The overarching hypothesis is that, by performing the above analyses for multiple AIPEX data sets collected during both RI and non-RI events, it will be possible to determine the conditions that are triggers for RI. This analysis strategy can also assist in the evaluation of 3-D numerical models, including the sufficiency (or lack thereof) of the horizontal resolution, and the microphysical and

planetary boundary layer parameterization schemes. Dropsonde, flight-level, super-obbed Doppler radar, and SFMR data are made available over the GTS and assimilated in real time, while full Doppler fields and lower fuselage radar will be available post-flight.

References:

Alvey, G.R. III, J. Zawislak, and E. Zipser, 2015: Precipitation Properties Observed during Tropical Cyclone Intensity Change. *Mon. Wea. Rev.*, **143**, 4476–4492. doi: 10.1175/MWR-D-15-0065.1.

Bhatia, K. T., and D. S. Nolan, 2013: Relating the skill of tropical cyclone intensity forecasts to the synoptic environment. *Wea. Forecasting*, **28**, 961–980, doi: 10.1175/WAF-D-12-00110.1.

DeMaria, M., C. R. Sampson, J. A. Knaff, and K. D. Musgrave, 2014: Is tropical cyclone intensity guidance improving? *Bull. Amer. Meteor. Soc.*, **95**, 387–398, doi:10.1175/BAMS-D-12-00240.1.

Gjorgjievska, S., and D. J. Raymond, 2014: Interaction between dynamics and thermodynamics during tropical cyclogenesis. *Atmos. Chem. and Phys.*, **14**, 3065–3082, doi:10.5194/ 784 acp-14-3065-2014.

Kaplan, J., M. DeMaria, and J. A. Knaff, 2010: A revised tropical cyclone rapid intensification index for the Atlantic and eastern North Pacific basins. *Wea. Forecasting*, **25**, 220–241, doi: 10.1175/2009WAF2222280.1.

Kaplan, J., and Coauthors, 2015: Evaluating environmental impacts on tropical cyclone rapid intensification predictability utilizing statistical models. *Wea. Forecasting*, **30**, 1374–1396, doi: 10.1175/WAF-D-15-0032.1.

Marks, F. D., Jr., R. A. Houze Jr., and J. F. Gamache, 1992: Dual-aircraft investigation of the inner core of Hurricane Norbert. Part I: Kinematic structure. *J. Atmos. Sci.*, **49**, 919–942, doi: 10.1175/1520-0469(1992)049<0919:DAIOTI>2.0.CO;2.

Nguyen, L. T., R. Rogers, and P. Reasor 2017: Thermodynamic and kinematic influences on precipitation symmetry in sheared tropical cyclones: Bertha and Cristobal (2014). *Mon. Wea. Rev.* In review.

Nolan, D. S., Y. Moon, and D. P. Stern, 2007: Tropical cyclone intensification from asymmetric convection: Energetics and efficiency. *J. Atmos. Sci.*, **64**, 3377–3405, doi: 10.1175/JAS3988.1.

Rappaport, E. N., and Coauthors, 2009: Advances and Challenges at the National Hurricane Center. *Wea. Forecasting*, **24**, 395–419.

Raymond, D. J., S. L. Sessions, and C. L. Carrillo, 2011: Thermodynamics of tropical cyclogenesis in the northwest pacific. *J. Geophys. Res. Atmos.*, **116** (D18), doi:10.1029/2011JD015624

Reasor, P. D., R. F. Rogers, and S. Lorsolo, 2013: Environmental flow impacts on tropical cyclone structure diagnosed from airborne Doppler radar composites. *Mon. Wea. Rev.*, **141**, 2949–2969, doi: 10.1175/MWR-D-12-00334.1.

Rogers, R., P. Reasor, and S. Lorsolo, 2013: Airborne Doppler observations of the inner-core structural differences between intensifying and steady-state tropical cyclones. *Mon. Wea. Rev.*, **141**, 2970–2991, doi: 10.1175/MWR-D-12-00357.1.

Rogers, R. F., P. D. Reasor, and J. A. Zhang, 2015: Multiscale structure and evolution of Hurricane Earl (2010) during rapid intensification. *Mon. Wea. Rev.*, **143**, 536–562, doi: 10.1175/MWR-D-14-00175.1.

Rogers, R., J. Zhang, J. Zawislak, H. Jiang, G. Alvey, E. Zipser, and S. Stevenson, 2016: Observations of the structure and evolution of Hurricane Edouard (2014) during intensity change. Part II: Kinematic structure and the distribution of deep convection. *Mon. Wea. Rev.*, **144**, 3355–3376, doi: 10.1175/MWR-D-16-0017.1.

Rozoff, C. M., and J. P. Kossin, 2011: New probabilistic forecast models for the prediction of tropical cyclone rapid intensification. *Wea. Forecasting*, **26**, 677–689, doi: 10.1175/WAF-D-10-05059.1.

Schubert, W. H., and J. J. Hack, 1982: Inertial stability and tropical cyclone development. *J. Atmos. Sci.*, **39**, 1687–1697, doi:10.1175/1520-0469(1982)039<1687:ISATCD>2.0.CO;2.

Tao, C., and H. Jiang, 2015: Distributions of shallow to very deep precipitation–convection in rapidly intensifying tropical cyclones. *J. Climate*, **28**, 8791–8824, doi: 10.1175/JCLI-D-14-00448.1.

Vigh, J. L., and W. H. Schubert, 2009: Rapid development of the tropical cyclone warm core. *J. Atmos. Sci.*, **66**, 3335–3350, doi: 10.1175/2009JAS3092.1.

Zawislak, J., H. Jiang, G. Alvey, E. Zipser, R. Rogers, J. Zhang, and S. Stevenson, 2016: Observations of the structure and evolution of Hurricane Edouard (2014) during intensity change. Part I: Relationship between the thermodynamic structure and precipitation. *Mon. Wea. Rev.*, **144**, 3333–3354, doi: 10.1175/MWR-D-16-0017.1.

Zhang, J. A., R. F. Rogers, P. Reasor, E. Uhlhorn, and F. D. Marks Jr., 2013: Asymmetric hurricane boundary layer structure from dropsonde composites in relation to the environmental wind shear. *Mon. Wea. Rev.*, **141**, 3968–3984, doi: 10.1175/MWR-D-12-00335.1.